nature plants

LETTERS

https://doi.org/10.1038/s41477-021-00858-5

Check for updates

Enhancing grain-yield-related traits by CRISPR–Cas9 promoter editing of maize *CLE* genes

Lei Liu[1], Joseph Gallagher[2], Edgar Demesa Arevalo[1], Richelle Chen[1], Tara Skopelitis[1], Qingyu Wu[1,3], Madelaine Bartlett[2] and David Jackson[1]✉

Several yield-related traits selected during crop domestication and improvement[1,2] are associated with increases in meristem size[3], which is controlled by CLE peptide signals in the CLAVATA–WUSCHEL pathway[4–13]. Here, we engineered quantitative variation for yield-related traits in maize by making weak promoter alleles of *CLE* genes, and a null allele of a newly identified partially redundant compensating *CLE* gene, using CRISPR–Cas9 genome editing. These strategies increased multiple maize grain-yield-related traits, supporting the enormous potential for genomic editing in crop enhancement.

Cereal crops such as maize provide our main sources of food and feed, and were domesticated from wild ancestors by the selection of favourable alleles to reshape plant and inflorescence architecture[1]. In maize, one of the most dramatic changes was in ear size, from a tiny ear with 6–12 kernels in the ancestor teosinte, to a massive ear with many hundreds of kernels in modern maize[1,2]. Ear size is determined during development[3], when the inflorescence meristems (IMs) proliferate to generate a stereotypical series of spikelet and floral meristems that form kernels after fertilization[3]. Therefore, kernel number per ear depends on IM activity, which is maintained by a CLAVATA (CLV)-WUSCHEL (WUS) feedback signalling pathway, first discovered in *Arabidopsis* but conserved in other species, including maize[4–9]. In this pathway, a homeodomain transcription factor, WUS, is expressed in the organizing centre of the meristem and promotes expression of the secreted peptide CLV3, which binds its receptor, CLV1 to repress *WUS* expression[4–9]. CLV orthologs in maize include THICK TASSEL DWARF1 (TD1, CLV1 ortholog)[10] and ZmCLAVATA3/EMBRYO SURROUNDING REGION-RELATED7 (ZmCLE7, CLV3 ortholog)[11,12], as well as a distinct CLE peptide, ZmFON2-LIKE CLE PROTEIN1 (ZmFCP1, CLV3 paralog)[13] that acts in a distinct CLV pathway to repress *WUS* expression. Mutations in *CLV* genes cause meristem over-proliferation, leading to enlarged inflorescence stems and fasciated ears in maize that develop many more disorganized and shorter kernel rows with low grain yield[10–14]. However, weak coding sequence alleles of *fasciated ear2* (*fea2*) and *fea3* generated by ethyl methanesulfonate mutagenesis cause a quantitative increase in kernel rows. These weak alleles maintain meristem organization and ear length, highlighting the potential to quantitatively manipulate *fea* genes for yield enhancement[13–15].

An alternative to generating weak alleles by targeting coding regions is to use CRISPR–Cas9 editing of *cis*-regulatory regions, such as promoters, as used in tomato to engineer quantitative variation for inflorescence traits[16]. Here we show that a similar strategy is successful in maize, a main global crop with a more complex genome organization and inflorescence architecture. We used CRISPR–Cas9 to edit maize *CLE* promoters and a newly characterized maize *CLE* gene identified through its compensatory upregulation in a *Zmcle7* mutant. Distal *cis*-regulatory variation largely reshaped plant and inflorescence morphology during maize domestication and improvement[17–22], and our results indicate that proximal promoter engineering can also modify traits quantitatively to enhance crop yields.

For *CLE* promoter mutagenesis, we expressed Cas9 with nine single-guide RNAs (sgRNAs) targeting promoter regions of roughly 2 kilobases (kb) for *ZmCLE7* (Fig. 1a) and roughly 1.1 kb for *ZmFCP1* (Fig. 1e). These sgRNA targeted regions included accessible chromatin regions in developing ears detected by ATAC-seq (assay for transposase-accessible chromatin using sequencing) and MNase-seq (micrococcal nuclease digestion with deep sequencing) (Fig. 1b,f)[23,24]. After transformation into maize, editing was identified by PCR amplification and Sanger sequencing. Six promoter-edited alleles for *ZmCLE7* and five for *ZmFCP1* were identified, including large deletions and inversions, and they were named $CLE7^{CR\text{-}pro1}$ to $CLE7^{CR\text{-}pro6}$ (Fig. 1c), and $FCP1^{CR\text{-}pro1}$ to $FCP1^{CR\text{-}pro5}$ (Fig. 1g). Lines carrying each allele were backcrossed twice with the B73 inbred line to standardize the genetic background and segregate away the Cas9 transgene to avoid further edits.

We first asked if promoter editing affected gene expression, by measuring transcript levels in dissected tips of developing ear primordia by quantitative PCR with reverse transcription (RT–qPCR). The $CLE7^{CR\text{-}pro1}$, $CLE7^{CR\text{-}pro2}$, $CLE7^{CR\text{-}pro4}$ and $CLE7^{CR\text{-}pro5}$ alleles all had deletions in accessible chromatin regions of their promoters (Fig. 1b,c), and significantly decreased *ZmCLE7* expression, by roughly 45 to 65% (Fig. 1d). In contrast, expression was not significantly changed in the $CLE7^{CR\text{-}pro6}$ allele, where less accessible chromatin was deleted, or in the $CLE7^{CR\text{-}pro3}$ allele, which carried an inversion (Fig. 1c). This inversion allele led to an expanded expression of *ZmCLE7* in developing ear primordia, from the normal epidermal-enriched expression towards the centre of the IM (Supplementary Fig. 1). All five $FCP1^{CR\text{-}pro}$ alleles had significantly lower *ZmFCP1* expression, and was lowest in $FCP1^{CR\text{-}pro2}$ with a roughly 69% reduced expression (Fig. 1e–h).

To evaluate the phenotype of each promoter-edited allele, heterozygous lines were crossed with their respective null alleles[11,13] in different genetic backgrounds, and ear traits scored in the F1 progeny families that segregated for the edited or control wild type allele, as in Rodriguez-Leal et al.[16] (Supplementary Fig. 2). As *ZmCLE7* and *ZmFCP1* control meristem size, we observed roughly 5 mm stage developing ear primordia in a subset of the alleles. *Zmcle7* null alleles have fasciated ears with massively enlarged IMs and very disordered spikelet rows[11], whereas two promoter deletion

[1]Cold Spring Harbor Laboratory, Cold Spring Harbor, NY, USA. [2]Biology Department, University of Massachusetts Amherst, Amherst, MA, USA. [3]Present address: Institute of Agricultural Resources and Regional Planning, Chinese Academy of Agricultural Sciences, Beijing, China. ✉e-mail: jacksond@cshl.edu

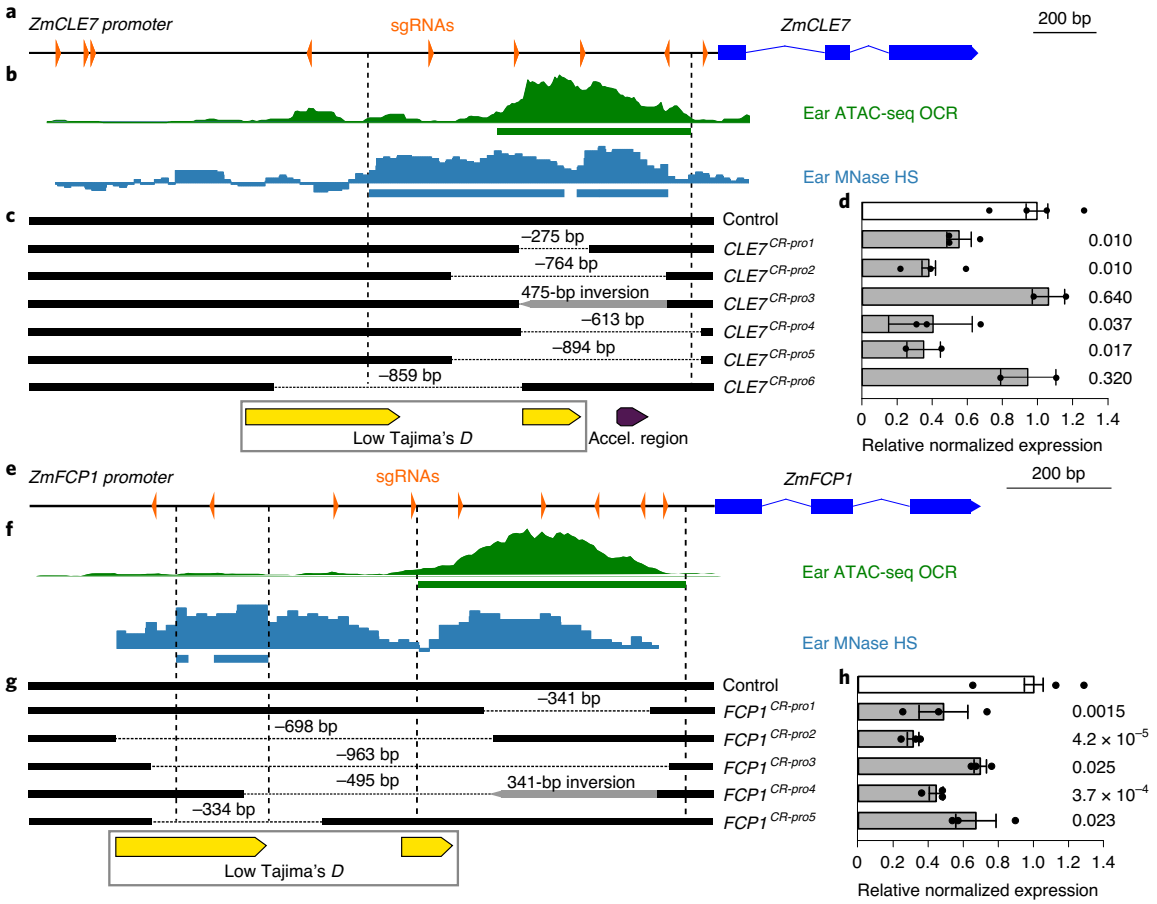

Fig. 1 | Mutation of *ZmCLE7* and *ZmFCP1* promoters by CRISPR–Cas9. a,**e**, The distribution of sgRNA target sites cover around 2 and 1.1 kb of the promoters of *ZmCLE7* (**a**) and *ZmFCP1* (**e**), respectively; orange arrowheads, sgRNAs; blue boxes, exons. **b**,**f**, The accessible chromatin regions of *ZmCLE7* (**b**) and *ZmFCP1* (**f**) promoters in developing maize ear primordia were detected by ATAC-seq[23] and MNase-seq[24]; green peaks, ATAC-seq peaks; green boxes, open chromatin regions (OCR) defined by ATAC-seq peaks; light-blue peaks, MNase-seq peaks; light-blue boxes, MNase hypersensitive sites (HS) defined by MNase-seq peaks; vertical dashed lines indicated the accessible chromatin regions. **c**,**g**, Six and five promoter-edited alleles of *ZmCLE7* (**c**) and *ZmFCP1* (**g**) were obtained, respectively. The deletion (−) and inversion base pairs are indicated by numbers, with regions of selection (yellow and purple arrows) below; yellow arrows, Low Tajima's *D* conserved regions, suggesting selection acting on promoter regions within the maize NAM diversity lines and other inbreds; the purple arrow, accelerated region from phyloP results, comparing evolution in maize and the grasses *Setaria italica*, *Setaria viridis*, *Oropetium thomaeum*, *Oryza sativa* and *Brachypodium distachyon*, indicates accelerated evolution in the grasses. **d**,**h**, The normalized relative expression of *ZmCLE7* (**d**) and *ZmFCP1* (**h**) in ear primordia of homozygous promoter-edited alleles and wild type controls were measured by RT-qPCR (three biological and three technical replicates), and normalized to *ZmActin*. The error bars represent standard error of the mean, and *P* values are listed (two-tailed, two-sample *t*-test).

alleles ($CLE7^{CR\text{-}pro1}$ and $CLE7^{CR\text{-}pro2}$) had more modestly enlarged IMs compared to control sibling plants (Fig. 2a,b), and the spikelet rows of $CLE7^{CR\text{-}pro1}$ were relatively straight compared to the *Zmcle7* null mutants (Fig. 2a). In contrast, the $CLE7^{CR\text{-}pro3}$ allele ear primordia appeared to be narrower than normal, but their IMs were not significantly different from the controls (Fig. 2a,b). We also measured IM sizes of the *ZmFCP1* promoter deletion alleles. However, they were all similar to their controls (Fig. 2c,d), as expected since the B73 genetic background partially suppresses the fasciated ear phenotype of *Zmfcp1* mutants[13].

At harvest, the fasciated ears of *Zmcle7* null alleles are highly disorganized and shorter with much lower grain yield (Supplementary Table 1). Notably, mature ears of all promoter-edited alleles were not fasciated and maintained regular ear architecture and kernel row organization (Fig. 3a)[11–13]. To evaluate the potential effect of promoter editing on grain production, we selected representative alleles and grew plants in the field under a randomized block design and scored eight yield-related traits. Two $CLE7^{CR\text{-}pro}$ deletion alleles showed a significant increase in most yield-related traits, including ear diameter, cob diameter, kernel row number, kernel depth, ear weight and grain yield per ear (Fig. 3a–i and Supplementary Table 1). Weak *fea* coding sequence alleles enhance kernel row number because larger IMs can initiate more rows[13,15], and in line with this, $CLE7^{CR\text{-}pro1}$ and $CLE^{CR\text{-}pro2}$ ears had roughly six more kernel rows than their sibling controls (Fig. 3a,b and Supplementary Table 1). Although these alleles produced slightly shorter ears, the striking increase in other yield-related traits resulted in significantly higher grain yields per ear, of roughly 14 to 26% (Fig. 3a–i and Supplementary Table 1). In contrast to these two $CLE7^{CR\text{-}pro}$ deletion alleles, the promoter inversion allele, $CLE7^{CR\text{-}pro3}$ had opposite effects on many yield-related traits, including reductions in kernel row number, ear and cob diameter and ear weight, leading to an approximately 18% decrease in grain yield per ear (Fig. 3a–i and Supplementary Table 1). This may be caused by the expansion of the *CLE7* expression domain in $CLE7^{CR\text{-}pro3}$ (Supplementary Fig. 1), which is predicted to reduce *WUS* expression and lead to a decrease in meristem size and yield-related traits. We confirmed the kernel row number changes of these three $CLE7^{CR\text{-}pro}$ alleles in a second field

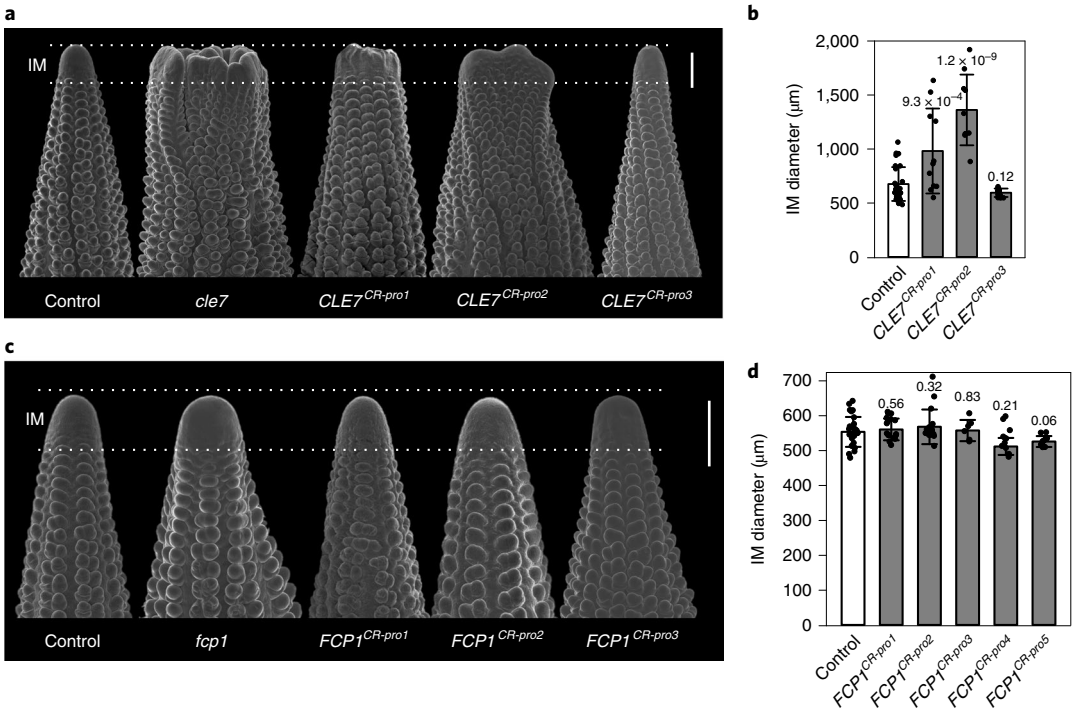

Fig. 2 | *ZmCLE7* promoter-edited alleles as heterozygotes with a null allele increase IM size. a, Scanning electron micrographs of representative developing ears from heterozygous *ZmCLE7* promoter-edited alleles/null (*CLE7*$^{CR\text{-}pro}$*/Zmcle7*), homozygous *cle7* null allele and the control (*+/Zmcle7*); the dashed lines mark the IMs. **b**, IM diameters of *ZmCLE7* promoter-edited alleles (*CLE7*$^{CR\text{-}pro}$*/Zmcle7*) and the control (*+/Zmcle7*) show that *CLE7*$^{CR\text{-}pro1}$ and *CLE7*$^{CR\text{-}pro2}$ have an enlarged IM compared to control; $n = 29$, 11, 10 and 10 for control, *CLE7*$^{CR\text{-}pro1}$, *CLE7*$^{CR\text{-}pro2}$ and *CLE7*$^{CR\text{-}pro3}$, respectively. **c**, Scanning electron micrographs of representative developing ears from heterozygous *ZmFCP1* promoter-edited alleles/null (*FCP1*$^{CR\text{-}pro}$*/Zmfcp1*), homozygous *fcp1* null allele and the control (*+/Zmfcp1*). **d**, IM diameters of *ZmFCP1* promoter-edited alleles and the control show no obvious changes in IM size of *FCP1*$^{CR\text{-}pro}$ alleles; $n = 14$, 17, 16, 6, 11 and 9 for control and *FCP1*$^{CR\text{-}pro1}$ to *FCP1*$^{CR\text{-}pro5}$, respectively. Scale bars, 500 μm. For **a** and **c**, ears from five plants of each genotype were imaged, with similar results. For **b** and **d**, data are presented as mean values ± s.d. The *P* values are listed above the histograms (two-tailed, two-sample *t*-test).

season and found that three additional *CLE7*$^{CR\text{-}pro}$ deletion alleles (*CLE7*$^{CR\text{-}pro4}$, *CLE7*$^{CR\text{-}pro5}$ and *CLE7*$^{CR\text{-}pro6}$), also significantly increased kernel row number (Supplementary Fig. 3a and Supplementary Table 1). We also scored yield-related traits in the *FCP1*$^{CR\text{-}pro2}$ allele, as it had the lowest *ZmFCP1* expression, and found that it significantly increased kernel row number, ear length, ear weight and grain yield per ear traits (Fig. 3j–q and Supplementary Table 2). The *CLE* promoter-edited alleles significantly increased kernel number, but their kernels appeared narrower than their controls (Fig. 3a,j). However, 100-kernel weight was not significantly decreased (Supplementary Tables 1 and 2), probably due to an increase in kernel depth (Fig. 3g,o and Supplementary Tables 1 and 2).

The high productivity of maize depends on heterosis for yield in hybrids[25], so we also crossed promoter-edited alleles to their respective null alleles in different genetic backgrounds, to create hybrids; B73×W22 for *CLE7*$^{CR\text{-}pro}$ and B73×A619 for *FCP1*$^{CR\text{-}pro}$ alleles (Methods). We scored four *CLE7*$^{CR\text{-}pro}$ alleles, and each led to changes in yield-related traits similar to in the inbred background; the promoter deletion alleles (*CLE7*$^{CR\text{-}pro2}$, *CLE7*$^{CR\text{-}pro4}$ and *CLE7*$^{CR\text{-}pro5}$) increased kernel row number, ear diameter, ear weight and grain yield per ear, and the *CLE7*$^{CR\text{-}pro3}$ promoter inversion allele decreased these traits (Supplementary Fig. 4a–h and Supplementary Table 1). From the five *FCP1*$^{CR\text{-}pro}$ alleles, *FCP1*$^{CR\text{-}pro2}$ and *FCP1*$^{CR\text{-}pro3}$ had significantly higher grain yield compared to their sibling controls, and these alleles had larger deletions and disruptions of regions of open chromatin (Supplementary Fig. 5 and Supplementary Table 2). *FCP1*$^{CR\text{-}pro2}$ plants had significant increases in kernel row number, ear length, kernel number per row and ear weight (Supplementary Fig. 5 and Supplementary Table 2), whereas *FCP1*$^{CR\text{-}pro3}$ had more modest increases that were significant only for kernel row number, kernel depth and ear weight (Supplementary Table 2), resulting in grain yield per ear increases of roughly 18.5 and 13.5%, respectively (Supplementary Fig. 5i and Supplementary Table 2). Three additional *FCP1*$^{CR\text{-}pro}$ alleles (*FCP1*$^{CR\text{-}pro1}$, *FCP1*$^{CR\text{-}pro4}$ and *FCP1*$^{CR\text{-}pro5}$) did not affect ear size or weight significantly (Supplementary Fig. 5 and Supplementary Table 2). We confirmed the increases in kernel row number in *CLE7*$^{CR\text{-}pro}$ and *FCP1*$^{CR\text{-}pro}$ alleles in an independent field season (Supplementary Fig. 3 and Supplementary Tables 1 and 2). Last, in addition to testing promoter-edited alleles in heterozygous combination with null alleles, we also tested their effect when homozygous. Similar to before (Fig. 3), the homozygous promoter deletion plants developed non-fasciated ears, with similar changes in kernel row numbers (Supplementary Figs. 6 and 7 and Supplementary Tables 1 and 2). We compared the kernel row number of these homozygous promoter deletion alleles plants to their heterozygotes combined with null alleles in the same genetic background and environment (B73 background, 2020 Kekaha, Hawaii). In some cases, the heterozygous promoter allele/null combination had a higher kernel row number than the homozygous promoter allele plants (for example, *CLE7*$^{CR\text{-}pro4}$, *CLE7*$^{CR\text{-}pro6}$ and *FCP1*$^{CR\text{-}pro2}$; $P = 7.23\times10^{-3}$, 3.01×10^{-7} and 2.12×10^{-12}, respectively), but in other cases they did not (Supplementary Tables 1 and 2). We also asked if plants heterozygous for a null allele could enhance yield-related traits, and found that this was the case for *Zmcle7*, where null allele heterozygotes had a higher kernel row number than wild-type siblings ($P = 6.16\times10^{-5}$). However, the effect size was less than for the promoter-edited alleles, and similar trait changes were not seen for *Zmfcp1* heterozygotes (Supplementary Tables 1 and 2). Apart from the increase in

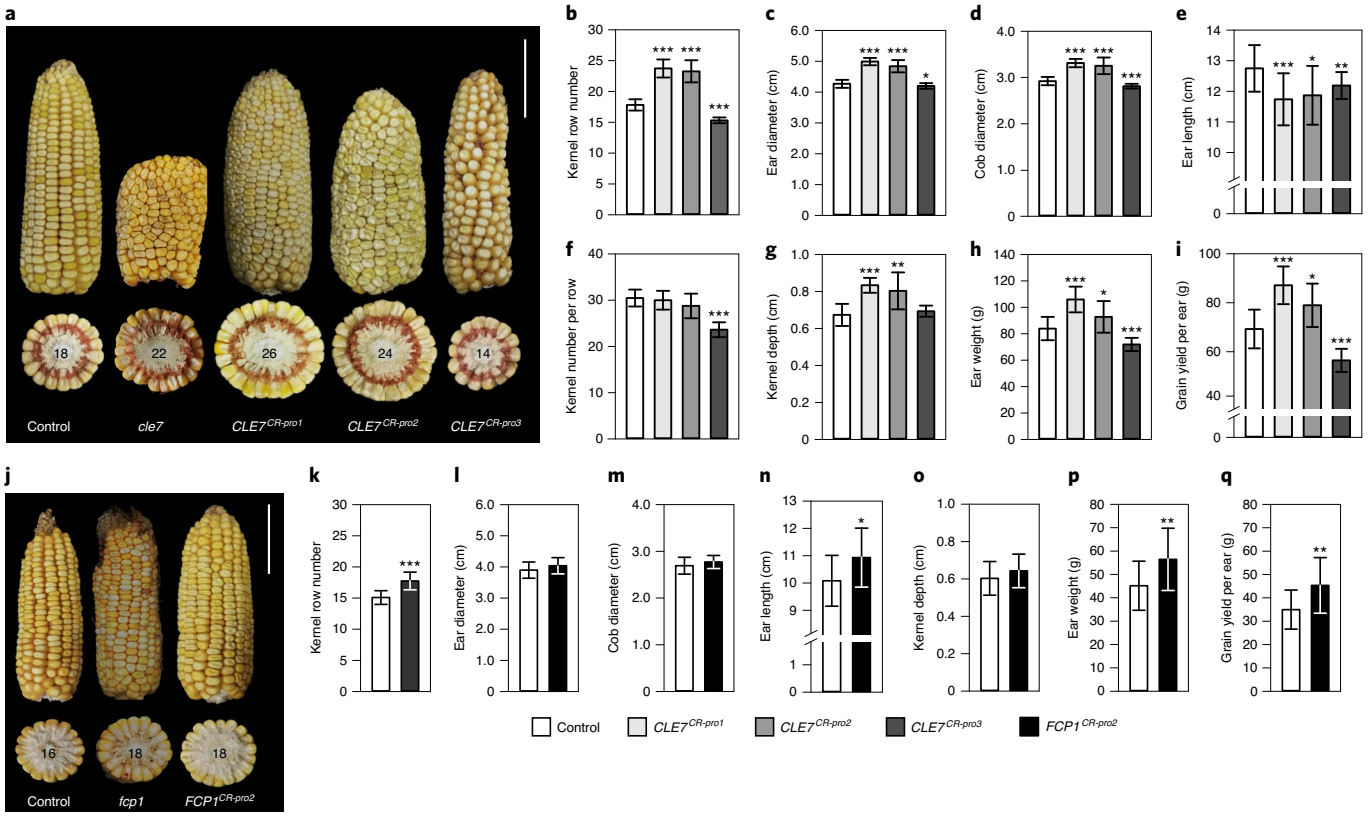

Fig. 3 | *ZmCLE7* and *ZmFCP1* promoter-edited alleles as heterozygotes with a null allele increase grain-yield-related traits by producing enlarged, non-fasciated ears. a, Representative mature ears of control (+/*Zmcle7*), homozygous *cle7* null allele and three heterozygous *ZmCLE7* promoter-edited alleles/null (*CLE7*$^{CR\text{-}pro}$/*Zmcle7*) show *CLE7*$^{CR\text{-}pro}$ alleles produce non-fasciated ears with obvious changes in size. **b**–**i**, Performance of *ZmCLE7* promoter-edited alleles in grain-yield-related traits including kernel row number (**b**, $P = 3.90\times10^{-15}$, 3.35×10^{-6} and 3.71×10^{-11}), ear diameter (**c**) ($P = 6.61\times10^{-20}$, 4.02×10^{-6} and 0.036), cob diameter (**d**) ($P = 4.54\times10^{-16}$, 1.78×10^{-4} and 4.90×10^{-5}), ear length (**e**) ($P = 2.58\times10^{-4}$, 0.0216 and 7.60×10^{-3}), kernel number per row (**f**) ($P = 0.22$, 0.064 and 7.28×10^{-11}), kernel depth (**g**) ($P = 3.43\times10^{-12}$, 4.60×10^{-3} and 0.087), ear weight (**h**) ($P = 9.05\times10^{-9}$, 0.044 and 2.05×10^{-5}) and grain yield per ear (**i**) ($P = 1.42\times10^{-8}$, 0.014 and 2.14×10^{-6}); white bar, sibling controls (+/*Zmcle7*), $n = 199$; grey bars represent *CLE7*$^{CR\text{-}pro1}$/*Zmcle7* ($n = 193$), *CLE7*$^{CR\text{-}pro2}$/*Zmcle7* ($n = 58$) and *CLE7*$^{CR\text{-}pro3}$/*Zmcle7* ($n = 98$). **j**, Representative mature ears of control (+/*Zmfcp1*), homozygous *fcp1* null allele and heterozygous *FCP1*$^{CR\text{-}pro2}$/null show enlarged but non-fasciated ear of *FCP1*$^{CR\text{-}pro2}$. **k**–**q**, Performance of *FCP1*$^{CR\text{-}pro2}$ in grain-yield-related traits including kernel row number (**k**) ($P = 5.49\times10^{-17}$), ear diameter (**l**) ($P = 0.085$), cob diameter (**m**) ($P = 0.13$), ear length (**n**) ($P = 0.013$), kernel depth (**o**) ($P = 0.25$), ear weight (**p**) ($P = 6.67\times10^{-3}$) and grain yield per ear (**q**) ($P = 4.54\times10^{-3}$); white bar, sibling controls (+/*Zmfcp1*), $n = 42$; black bar, *FCP1*$^{CR\text{-}pro2}$/*Zmfcp1*, $n = 58$. For **b**–**i** and **k**–**q**, data are presented as mean values ± s.d. $^*P \le 0.05$, $^{**}P \le 0.01$, $^{***}P \le 0.001$, from a two-tailed, two-sample *t*-test. Scale bar, 5 cm. The values are listed in Supplementary Tables 1 (**b**–**i**) and 2 (**k**–**q**).

grain-yield-related traits, the promoter-edited alleles had no obvious effect on other important agronomic traits, including plant height, ear height and tassel branch number, and affected tassel length in *FCP1*$^{CR\text{-}pro2}$ only slightly (Supplementary Fig. 8 and Supplementary Tables 1 and 2). In summary, promoter editing of *ZmCLE7* and *ZmFCP1* can generate new alleles that enhance grain-yield-related traits, and can in rare cases, as in *CLE7*$^{CR\text{-}pro3}$, produce opposite effects on phenotype, presumably reflecting a gain of function that may be beneficial for the engineering of certain other traits, for example decreasing ear diameter to increase ear drying-rate[26].

Fig. 4 | *ZmCLE1E5* CRISPR null alleles enhance meristem size and grain-yield-related traits. a, Three maize *CLE* genes, *ZmCLE7*, *ZmFCP1* and *ZmCLE1E5* were upregulated in developing ear tips of *Zmcle7* mutants; RNA-seq fold changes were calculated by the fragments per kilobase of transcript per million of these genes in the *Zmcle7* mutant relative to the control (two biological replicates). **b**–**d**, *ZmCLE1E5* is expressed in the tips of developing ear meristems (mRNA in situ hybridization); the experiment was performed twice with similar results, using ears from at least three independent plants per experiment. **b**, IM. **c**, Spikelet meristem. **d**, Negative control using sense probe. Scale bars, 100 μm. **e**–**h**, Scanning electron micrographs of representative developing ears from control (homozygous wild-type siblings); ears from five plants of each genotype were imaged, with similar results (**e**), *Zmcle1e5-cr2* (**f**), *Zmcle7* (**g**) and *Zmcle7;Zmcle1e5-cr2* double mutants (**h**). Scale bars, 500 μm. IMs are outlined by dashed lines. **i**, *Zmcle1e5-cr2* mutants have wider IMs and significantly enhance *Zmcle7*; graphed are IM diameters of control ($n = 23$), *Zmcle1e5-cr2* (*cle1e5*, $n = 24$), *Zmcle7* (*cle7*, $n = 12$) and *Zmcle7;Zmcle1e5-cr2* double mutants (*cle7;cle1e5*, $n = 16$); *P* values as indicated, from a two-tailed, two-sample *t*-test. **j**, Representative mature ears of control and *Zmcle1e5-cr1* mutants show enlarged but non-fasciated ear of *Zmcle1e5-cr1*; Scale bar, 5 cm. **k**–**r**, *Zmcle1e5-cr1* mutants enhance yield-related traits, including kernel row number (**k**) ($P = 0.043$), ear diameter (**l**) ($P = 0.041$), cob diameter (**m**) ($P = 0.049$), ear length (**n**) ($P = 1.10\times10^{-4}$), kernel number per row (**o**) ($P = 3.90\times10^{-3}$), kernel depth (**p**) ($P = 8.20\times10^{-3}$), ear weight (**q**) ($P = 3.80\times10^{-3}$) and grain yield per ear (**r**) ($P = 8.60\times10^{-5}$); white bar, sibling controls, $n = 11$; grey bar, *Zmcle1e5-cr1*, $n = 15$. $^*P \le 0.05$, $^{**}P \le 0.01$, $^{***}P \le 0.001$, from a two-tailed, two-sample *t*-test. For **i** and **k**–**r**, data are presented as mean values ± s.d. The values for **k**–**r** are listed in Supplementary Table 3.

We next asked whether the promoter alleles encompassed regions of evolutionary conservation or acceleration within the grasses, and thus might represent regions of shared or divergent function. For *ZmCLE7*, mVISTA analysis[27] found conserved regions only within the gene body (Supplementary Fig. 9a). A model-based assessment of non-coding sequence evolution in which the substitution rate in a region of interest is compared to a neutral model[28,29] produced similar results. However, this method also revealed sites of evolutionary acceleration, that is excessive substitution relative to the neutral model[28], within the grasses. This evolutionary acceleration suggests positive selection acting on the regulation of *ZmCLE7*. In contrast, mVISTA and model-based analyses showed conservation of the region surrounding *ZmFCP1*, indicating that its proximal regulatory regions are shared with other grasses (Supplementary Fig. 10a).

We further examined conservation within maize, by comparing the regions surrounding *ZmCLE7* and *ZmFCP1* in diverse maize lines[30,31]. We identified and aligned *ZmCLE7* and *ZmFCP1* orthologs within these genomes and calculated two related statistics: Tajima's

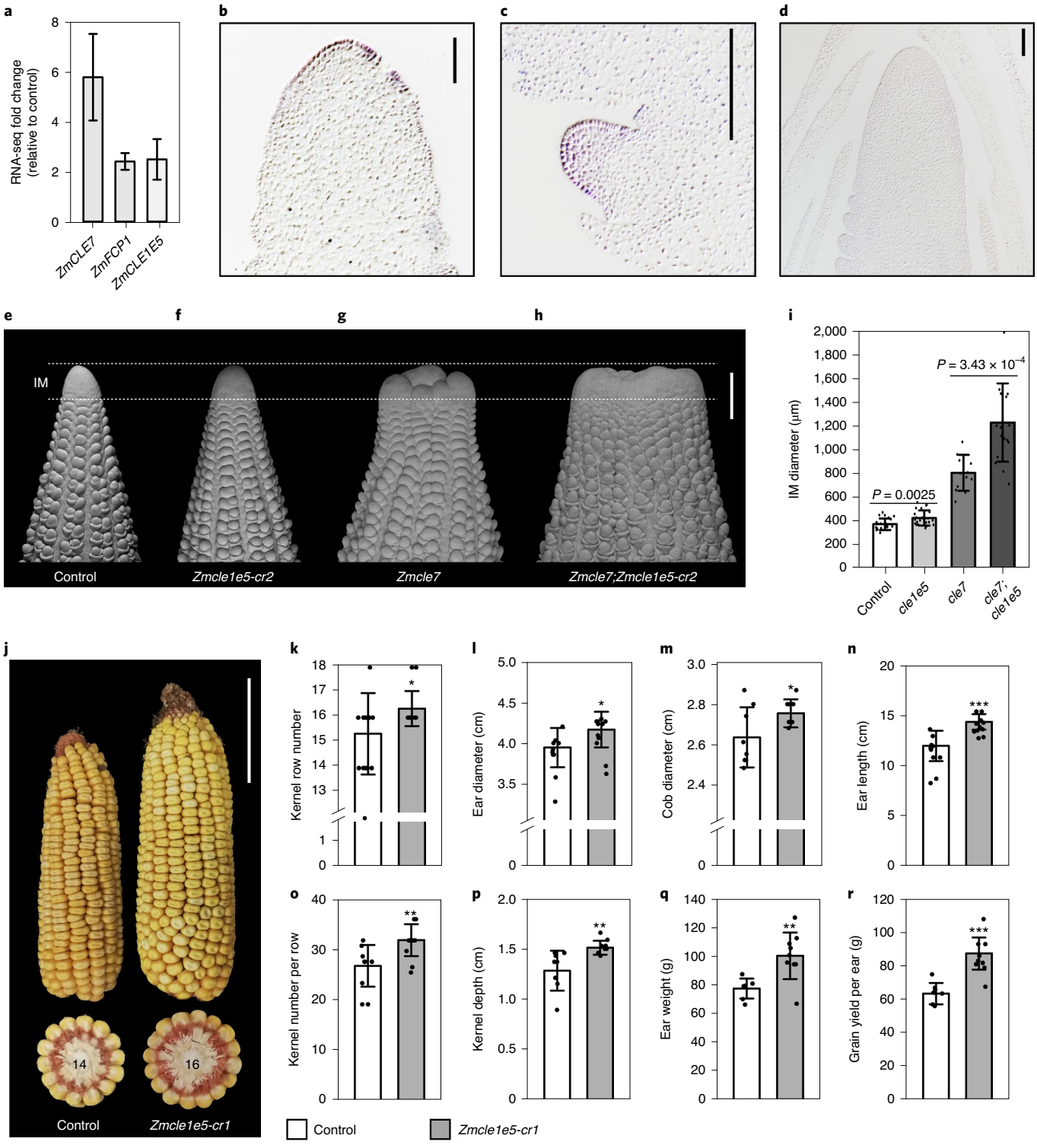

D and π, to assess selection[32]. π is a measure of nucleotide diversity, while Tajima's *D* is a statistic that uses π to test the null hypothesis of neutral evolution. Tajima's *D* and π were both lower in two regions upstream of *ZmCLE7* and one region directly downstream of it (Supplementary Fig. 9b), indicating conservation within maize, and suggesting selection. One of these conserved regions was tightly linked with the grass accelerated region (Supplementary Fig. 9a). Thus, these regions might jointly represent a new regulatory site within maize. We also found two regions upstream of *ZmFCP1* with negative Tajima's *D* and low nucleotide diversity, again possibly representing selection (Supplementary Fig. 9b and 10b). Together, our analyses suggest conservation of *ZmFCP1* regulation but divergence of *ZmCLE7* regulation among the grasses, and *ZmCLE7* promoter regulation is probably conserved within maize (Supplementary Fig. 9). Parts of the conserved and accelerated regions overlap with accessible chromatin regions (Fig. 1). Our promoter-edited alleles with disruptions in these overlapping regions produced large phenotypic changes, suggesting these regions are functional; however, this needs to be confirmed by analysis of more alleles. While the relationship between non-coding regions and phenotype is complex[16], the overlap between the evolutionarily conserved and accelerated regions and the phenotypically impactful promoter lesions highlights the value in identifying these regions.

In addition to *ZmCLE7* and *ZmFCP1*, another 47 *CLE* genes are annotated in maize, and many are expressed in shoot tissues[33]. To ask whether any act in meristem maintenance similar to *ZmCLE7* and *ZmFCP1* (refs. [11–13]), we took advantage of the fact that compensating genes are frequently upregulated when one functional paralog is mutated[11]. In a previous study, we found that *ZmFCP1* was upregulated in *Zmcle7* mutants[11]; however, in repeating this profiling experiment with deeper sequence coverage to detect lower expressed *CLE* genes, we found that *ZmCLE1E5*, from a closely related group, was also upregulated (Fig. 4a). Using messenger RNA in situ hybridization, we found expression of this gene predominantly in the epidermal and subepidermal layer of inflorescence and spikelet meristems (Fig. 4b–d), similar to *ZmCLE7* (Supplementary Fig. 1a), supporting the idea that it acts redundantly. To test this, we targeted the *ZmCLE1E5* coding sequence with CRISPR–Cas9 and two sgRNAs, and obtained two independent alleles: *Zmcle1e5-cr1* with a C deletion at the first sgRNA site, and *Zmcle1e5-cr2* with a T insertion at the second sgRNA site (Supplementary Fig. 11). Both alleles produced frameshifts before the functional CLE motif, and were therefore considered null alleles. After backcrossing to generate Cas9-free segregating families, we measured IMs of developing *Zmcle1e5* ears, as well as of *Zmcle7;Zmcle1e5* double mutants. As expected by the compensatory expression of *Zmcle1e5*, the mutants had significantly wider meristems, and greatly enhanced the fasciated phenotype of *Zmcle7* mutants, supporting the idea that *Zmcle1e5* acts as a partially redundant compensator of *Zmcle7* (Fig. 4e–i). Notably, unlike *Zmcle7* (ref. [11]), *Zmcle1e5* null mutant ears were not fasciated (Fig. 4j and Supplementary Fig. 12a), so we grew them in different environments to measure yield-related traits. Indeed, we found that both alleles could increase kernel row number, ear length, kernel number per row, ear diameter, cob diameter, kernel depth, ear weight and grain yield per ear, and 100-kernel weight did not significantly decrease (Fig. 4k–r, Supplementary Fig. 12b–i and Supplementary Table 3). Apart from the increase in grain-yield-related traits, *Zmcle1e5* null alleles had no obvious effect on other important agronomic traits, including plant height, ear height and tassel branch number, and affected tassel length slightly (Supplementary Fig. 8 and Supplementary Table 3). Our results indicate that *ZmCLE1E5* controls meristem development as a partially redundant compensator for *ZmCLE7*, and a null allele could significantly enhance grain yield per ear by making longer and wider ears with more kernels (Supplementary Table 3). Our results illustrate how knowledge of expression compensation, which is easy to assay, can be exploited to predict redundancy. Further, null alleles of this partially redundant compensator produced quantitative variation similar to weak promoter alleles of *ZmCLE7*, suggesting a new editing strategy for enhancing crop traits.

Grain yield is a complex trait, and linkage mapping and genome-wide association analyses have identified hundreds of quantitative trait loci (QTL) underlying maize yield-related traits (www.maizegdb.org/qtl). Most of these have a minor effect, and only a limited number have been cloned, including kernel row number QTL *KRN4* (ref. [22]), kernel weight QTL *qHKW1* (ref. [34]) and kernel number per row QTL *KNR6* (ref. [35]). These QTLs may have considerable effect, but only in some genetic backgrounds, for example, the beneficial allele of *KRN4* adds roughly 2.2 kernel rows in the H21 line, but only around 0.7 rows in Mo17 (ref. [22]). Moreover, for some potential yield genes, beneficial alleles may not exist, either because they did not arise naturally, or were lost along with the reduction of diversity during the domestication bottleneck[36,37]. The three *CLE* genes in this study are not linked to yield-related QTLs in the maize nested association mapping (NAM) populations[36], and we found that *ZmCLE7* regulatory regions have low variation within maize. Thus, new beneficial alleles created by CRISPR–Cas9 genome editing, based on knowledge about target genes including analyses of regulatory sequence evolution, reveals untapped genetic potential. We found that multiple promoter deletions of *ZmCLE7* and *ZmFCP1* produced enlarged ears with yield-related trait enhancement greater than cloned QTLs[22,34,35]. A trade-off between kernel number and weight was not observed in these alleles, as kernel weight was maintained while kernel number increased significantly. Thus, genome editing of *cis*-regulatory regions can quantitatively adjust expression level or pattern to enhance meristem activity and grain yield. In this study, we focused on alleles with large deletions or rearrangements, as such variation usually underlies maize QTL[22,34,35]. However, it is likely that editing of a few critical nucleotides in regulatory elements could also lead to substantial phenotype changes.

In addition to weak allele promoter editing, we also exploited the partial compensation among paralogs in the CLV-WUS feedback loop that is critical for stem cell homeostasis and phenotypic buffering[11]. We identified *ZmCLE1E5* as a partial *ZmCLE7* compensator, and found that CRISPR null alleles had much less severe meristem size phenotypes than *Zmcle7* (ref. [11]), but significantly enhanced it. *ZmCLE1E5* null alleles also quantitatively enhanced grain-yield-related traits, suggesting a potential use in crop improvement. In summary, we highlight two distinct ways in which genome editing can enhance maize traits, through CRISPR-based promoter fine tuning or by exploitation of compensation and redundancy mechanisms, which are probably applicable to diverse crops.

Methods

Genomic editing of maize *CLE*s by CRISPR–Cas9. CRISPR–Cas9 was used to create mutations in the promoter regions of *ZmFCP1* and *ZmCLE7*, and to generate null alleles for *ZmCLE1E5* (GRMZM2G434380). sgRNAs were designed based on the B73 reference genome by the CRISPR-P 2.0 web-tool[38]. sgRNA arrays were synthesized and cloned into a pGW-Cas9 construct, and transformed into maize Hi-II via *Agrobacterium*-mediated transformation[39]. Genomic edits were screened by PCR-amplifying and Sanger sequencing of the target regions. As Hi-II is an F1 hybrid line of two parents derived from A188 × B73, the *Cas9* negative edited plants were backcrossed to B73 for two generations to purify the genetic background before further phenotypic scoring and expression analysis. The guide RNA sequences for *ZmFCP1*, *ZmCLE7* and *ZmCLE1E5* and primers for promoter-edited alleles and *ZmCLE1E5* allele genotyping are listed in Supplementary Table 4.

Gene expression analysis. For promoter-edited alleles of *ZmCLE7* and *ZmFCP1*, named as $CLE7^{CR\text{-}pro}$ and $FCP1^{CR\text{-}pro}$, the homozygous edited plants and their wild type controls were screened from segregating populations and roughly 5 mm of ear primordia were collected and fixed in acetone, 10–20 plants for each biological replicate and three biological replicates for each. Next, the IM region was dissected and the RNA was extracted using Direct-zol RNA Miniprep Kit (Zymo Research), according to the manufacturer's instructions. A reverse transcription reaction was carried out by SuperScript III Reverse Transcriptase (Thermo Fischer Scientific),

and expression levels were measured by real-time qPCR using Universal SybrGreen Master Mix (Bio-Rad) on the CFX96 Real-Time System (Bio-Rad). The *ZmActin* gene was used as control. The primers used for quantitative real-time PCR are listed in Supplementary Table 4.

mRNA in situ hybridization was used to characterize the expression domains of *ZmCLE7* and *ZmCLE1E5* using fixed and embedded developing ears (5 mm) following a previously described protocol[40]. The primers used to prepare the probes for in situ hybridization are listed in Supplementary Table 4. To find *CLE* genes upregulated in *Zmcle7*, we dissected IMs tip (approximately 0.5 mm) from *Zmcle7* mutants and sibling controls from a segregating population, from around 5 mm developing ear primordia, 10–20 plants for each biological replicate and two biological replicates for each. Total RNA was extracted using the Direct-zol RNA Kit (Zymo Research) and sequenced on the NextSeq 500 platform (Illumina) at the Cold Spring Harbor Laboratory Genome Centre. Raw RNA-sequencing (RNA-seq) reads (on average, approximately 30 million reads for each) were trimmed with Trimmomatic v.0.36 (ref. [41]) (parameters: ILLUMINACLIP:TruSeq3-PE.fa:2:30:10:LEADING:3 TRAILING:3 SLIDINGWINDOW:4:20 MINLEN:50) and then aligned to B73 RefGen_v3 reference using TopHat v.2.1.1 (ref. [42]) (parameters –b2-sensitive–read-mismatches 2–read-edit-dist 2–min-anchor 8–splice-mismatches 0–min-intron-length 50–max-intron-length 50,000–max-multihits 20). Next, Cufflinks v.2.2.1 (ref. [43]) was used to calculate the gene expression levels and call differentially expressed genes.

Evaluation of grain-yield-related traits. Promoter-edited alleles were phenotyped as heterozygotes with a null allele, as proposed by Rodriguez-Leal et al.[16] (Supplementary Fig. 2). This strategy makes testing in a hybrid background more efficient, because we only need to introgress a single null allele, rather than all promoter-edited alleles, into a different genetic background. The heterozygous promoter-edited plants were crossed with their null allele to generate segregating populations, promoter-edited/null allele and wild type/null allele (control) offspring (Supplementary Fig. 2). The $CLE7^{CR\text{-}pro}$ and $FCP1^{CR\text{-}pro}$ alleles were backcrossed two times with the B73 inbred background. Null alleles of *Zmcle7*, three times backcrossed with B73 from Hi-II (ref. [11]) and in the W22 inbred background (from UniformMu, stock ID UFMu-02841) were crossed with $CLE7^{CR\text{-}pro}$ alleles to score grain-yield-related traits in inbred (B73) and hybrid (B73 × W22) backgrounds. Null alleles of *Zmfcp1* (ref. [13]) four times backcrossed with B73 or A619 were crossed with $FCP1^{CR\text{-}pro}$ alleles to score grain-yield-related traits in inbred (B73) and hybrid (B73 × A619) backgrounds. The homozygous $CLE7^{CR\text{-}pro}$ or $FCP1^{CR\text{-}pro}$ alleles and their wild-type sibling controls in the B73 background were also scored. For yield-related traits, mature ears were harvested and dried. Eight yield-related traits were scored, including ear length, kernel number per row, ear diameter, cob diameter, kernel row number, kernel depth, ear weight and grain yield per ear. The plants were grown under a randomized block design in field locations in Cold Spring Harbor (40° 51′ N 73° 27′ W), NY or Lloyd Harbor (40° 54′ N 73° 28′ W), NY (June to October) or Kekaha (21° 58′ N 159° 44′ W), HI (November to March), in a low density trial with 20–25 cm between plants in the same row. The rows were planted in pairs with around 50 cm between rows and 120 cm between pairs of rows. As *Zmcle1e5-cr1* and *cr2* were null alleles, homozygous *Zmcle1e5* and wild type controls from F2 segregating populations were used to score yield-related traits. Phenotyping of *Zmcle1e5* alleles was conducted in two independent field locations, Cold Spring Harbor, NY or Lloyd Harbor, NY (June to October) in 2019 and 2020, and Cold Spring Harbor, NY (January to May) in 2020. Detailed information of genetic backgrounds, environments, number of plants and statistical analysis for grain-yield-related traits of $CLE7^{CR\text{-}pro}$, $FCP1^{CR\text{-}pro}$ and *Zmcle1e5* alleles is listed in Supplementary Tables 1–3.

IM size measurement. A previous study found that the IM size of 5–15 mm developing ear primordia is significantly correlated with kernel row number in diverse maize inbred lines[15], so we dissected and imaged roughly 5 mm developing ear primordia a Leica DMRB microscope and Leica Micro publisher 5.9 RTV digital camera system and IM size was measured with ImageJ. A Hitachi S-3500N scanning electron microscope was used to take images of fresh ears. As the *Zmfcp1* null allele fasciated ear phenotype was suppressed in the B73 background[11], IM size measurements for $FCP1^{CR\text{-}pro}$ alleles were in the B73 × A619 background.

Evolutionary analysis. Orthologs of *ZmCLE7* and *ZmFCP1* were retrieved from Goad et al.[33]. These genes and 10 kb regions up and downstream were extracted from respective genomes using bedtools[44,45]. Conserved regions were called using mVISTA with default settings (70% similarity and minimum size of 50 bp)[26]. The same regions were aligned via MAFFT[46] and analysed with phyloP from the PHAST suite[27,28]. Orthogroups were called between all genomes using Orthofinder2 (ref. [47]). Genes from single-copy orthogroups were aligned and concatenated using SequenceMatrix[48]. The concatenated alignment was used to build a model with phyloFit in the PHAST suite[27]. The alignments of the *ZmCLE7* and *ZmFCP1* were analysed with phyloP using the conservation–acceleration model to test for conservation and acceleration concurrently[27,28]. Orthologous regions of *ZmCLE7* and *ZmFCP1* were extracted from maize NAM genomes and aligned with MUSCLE[49]. Alignments were analysed for Tajima's D and π per bp in TASSEL5 (ref. [50]) to assess selection[51]. Graphs were made in R[52].

Statistical analysis. The numbers of plants (n) are presented in the figure legends and shown in Supplementary Tables 1–3. Statistical calculations were performed using data from each individual plant. The two-tailed, two-sample Student's t-test was used to determine whether the average performance of each CRISPR edited allele was significantly different from its matched sibling controls.

Biological materials. All the maize lines used in this study are available upon request from the corresponding author.

Reporting Summary. Further information on research design is available in the Nature Research Reporting Summary linked to this article.

Data availability

The sequences of *ZmFCP1* and *ZmCLE7* promoter-edited alleles are listed in Supplementary Table 4. The RNA-seq datasets are available from the National Center for Biotechnology Information; the BioProject and SRA accession numbers are PRJNA494874 and SRR12616467–SRR12616470. Source data are provided with this paper.

Received: 4 September 2020; Accepted: 21 January 2021;
Published online: 22 February 2021

References

1. Doebley, J. F., Gaut, B. S. & Smith, B. D. The molecular genetics of crop domestication. *Cell* **127**, 1309–1321 (2006).
2. Doebley, J. F. The genetics of maize evolution. *Annu. Rev. Genet.* **38**, 37–59 (2004).
3. Vollbrecht, E. & Schmidt, R. J. in *Handbook of Maize: Its Biology* (eds Bennetzen, J. L & Hake, S. C.) 13–40 (Springer, 2009).
4. Wu, Q., Xu, F. & Jackson, D. All together now, a magical mystery tour of the maize shoot meristem. *Curr. Opin. Plant Biol.* **45**, 26–35 (2018).
5. Clark, S. E., Williams, R. W. & Meyerowitz, E. M. The *CLAVATA1* gene encodes a putative receptor kinase that controls shoot and floral meristem size in *Arabidopsis*. *Cell* **62**, 575–585 (1997).
6. Fletcher, J. C. Signaling of cell fate decisions by CLAVATA3 in *Arabidopsis* shoot meristems. *Science* **283**, 1911–1914 (1999).
7. Jeong, S., Trotochaud, A. E. & Clark, S. E. The *Arabidopsis CLAVATA2* gene encodes a receptor-like protein required for the stability of the CLAVATA1 receptor-like kinase. *Plant Cell* **11**, 1925–1933 (1999).
8. Brand, U., Fletcher, J. C., Hobe, M., Meyerowitz, E. M. & Simon, R. Dependence of stem cell fate in *Arabidopsis* on a feedback loop regulated by CLV3 activity. *Science* **289**, 617–619 (2000).
9. Schoof, H. et al. The stem cell population of *Arabidopsis* shoot meristems is maintained by a regulatory loop between the *CLAVATA* and *WUSCHEL* genes. *Cell* **100**, 635–644 (2000).
10. Bommert, P. et al. *thick tassel dwarf1* encodes a putative maize ortholog of the *Arabidopsis* CLAVATA1 leucine-rich repeat receptor-like kinase. *Development* **132**, 1235–1245 (2005).
11. Rodríguez-Leal, D. et al. Evolution of buffering in a genetic circuit controlling plant stem cell proliferation. *Nat. Genet.* **51**, 786–792 (2019).
12. Tran, Q. H. et al. Mapping-by-sequencing via MutMap identifies a mutation in Zmcle7 underlying fasciation in a newly developed EMS mutant population in an elite tropical maize inbred. *Genes* **11**, 281 (2020).
13. Je, B. I. et al. Signaling from maize organ primordia via FASCIATED EAR3 regulates stem cell proliferation and yield traits. *Nat. Genet.* **48**, 785–791 (2016).
14. Taguchi-Shiobara, F., Yuan, Z., Hake, S. & Jackson, D. The *fasciated ear2* gene encodes a leucine-rich repeat receptor-like protein that regulates shoot meristem proliferation in maize. *Genes Dev.* **15**, 2755–2766 (2001).
15. Bommert, P., Nagasawa, N. S. & Jackson, D. Quantitative variation in maize kernel row number is controlled by the *FASCIATED EAR2* locus. *Nat. Genet.* **45**, 334–337 (2013).
16. Rodríguez-Leal, D., Lemmon, Z. H., Man, J., Bartlett, M. E. & Lippman, Z. B. Engineering quantitative trait variation for crop improvement by genome editing. *Cell* **171**, 470–480 (2017).
17. Studer, A., Zhao, Q., Ross-Ibarra, J. & Doebley, J. Identification of a functional transposon insertion in the maize domestication gene *tb1*. *Nat. Genet.* **43**, 1160–1163 (2011).
18. Wills, D. M. et al. From many, one: genetic control of prolificacy during maize domestication. *PLoS Genet.* **9**, e1003604 (2013).
19. Salvi, S. et al. Conserved noncoding genomic sequences associated with a flowering-time quantitative trait locus in maize. *Proc. Natl Acad. Sci. USA* **104**, 11376–11381 (2007).
20. Hung, H.-Y. et al. *ZmCCT* and the genetic basis of day-length adaptation underlying the postdomestication spread of maize. *Proc. Natl Acad. Sci. USA* **109**, E1913–E1921 (2012).
21. Yang, Q. et al. CACTA-like transposable element in *ZmCCT* attenuated photoperiod sensitivity and accelerated the postdomestication spread of maize. *Proc. Natl Acad. Sci. USA* **110**, 16969–16974 (2013).

22. Liu, L. et al. *KRN4* controls quantitative variation in maize kernel row number. *PLoS Genet.* **11**, e1005670 (2015).
23. Sun, Y. et al. 3D genome architecture coordinates *trans* and *cis* regulation of differentially expressed ear and tassel genes in maize. *Genome Biol.* **21**, 143 (2020).
24. Parvathaneni, R. K. et al. The regulatory landscape of early maize inflorescence development. *Genome Biol.* **21**, 165 (2020).
25. Shull, G. H. The composition of a field of maize. *Am. Breed. Assoc. Rep.* **4**, 296–301 (1908).
26. Cross, H. Z. A selection procedure for ear drying-rates in maize. *Euphytica* **34**, 409–418 (1985).
27. Frazer, K. A., Pachter, L., Poliakov, A., Rubin, E. M. & Dubchak, I. VISTA: computational tools for comparative genomics. *Nucleic Acids Res.* **32**, W273–W279 (2004).
28. Siepel, A., Pollard, K. S. & Haussler, D. in *Research in Computational Molecular Biology* (eds Apostolico, A., et al.) 190–205 (Springer, 2006).
29. Cooper, G. M. et al. Distribution and intensity of constraint in mammalian genomic sequence. *Genome Res.* **15**, 901–913 (2005).
30. McMullen, M. D. et al. Genetic properties of the maize nested association mapping population. *Science* **325**, 737–740 (2009).
31. Gage, J. L., Monier, B., Giri, A. & Buckler, E. S. Ten years of the maize nested association mapping population: impact, limitations, and future directions. *Plant Cell* **32**, 2083–2093 (2020).
32. Tajima, F. Statistical method for testing the neutral mutation hypothesis by DNA polymorphism. *Genetics* **123**, 585–595 (1989).
33. Goad, D. M., Zhu, C. & Kellogg, E. A. Comprehensive identification and clustering of *CLV3/ESR-related* (*CLE*) genes in plants finds groups with potentially shared function. *N. Phytol.* **216**, 605–616 (2017).
34. Yang, N. et al. Genome assembly of a tropical maize inbred line provides insights into structural variation and crop improvement. *Nat. Genet.* **51**, 1052–1059 (2019).
35. Jia, H. et al. A serine/threonine protein kinase encoding gene *KERNEL NUMBER PER ROW6* regulates maize grain yield. *Nat. Commun.* **11**, 988 (2020).
36. Brown, P. J. et al. Distinct genetic architectures for male and female inflorescence traits of maize. *PLoS Genet.* **7**, e1002383 (2011).
37. Yamasaki, M. et al. A large-scale screen for artificial selection in maize identifies candidate agronomic loci for domestication and crop improvement. *Plant Cell* **17**, 2859–2872 (2005).
38. Liu, H. et al. CRISPR-P 2.0: an improved CRISPR–Cas9 tool for genome editing in plants. *Mol. Plant* **10**, 530–532 (2017).
39. Char, S. N. et al. An *Agrobacterium*-delivered CRISPR/Cas9 system for high-frequency targeted mutagenesis in maize. *Plant Biotechnol. J.* **15**, 257–268 (2017).
40. Jackson, D., Veit, B. & Hake, S. Expression of maize KNOTTED1 related homeobox genes in the shoot apical meristem predicts patterns of morphogenesis in the vegetative shoot. *Development* **120**, 405–413 (1994).
41. Bolger, A. M., Lohse, M. & Usadel, B. Trimmomatic: a flexible trimmer for Illumina sequence data. *Bioinformatics* **30**, 2114–2120 (2014).
42. Kim, D. et al. TopHat2: accurate alignment of transcriptomes in the presence of insertions, deletions and gene fusions. *Genome Biol.* **14**, R36 (2013).
43. Trapnell, C. et al. Transcript assembly and quantification by RNA-seq reveals unannotated transcripts and isoform switching during cell differentiation. *Nat. Biotechnol.* **28**, 511–515 (2010).
44. Goodstein, D. M. et al. Phytozome: a comparative platform for green plant genomics. *Nucleic Acids Res.* **40**, D1178–D1186 (2011).
45. Quinlan, A. R. BEDTools: the Swiss-Army tool for genome feature analysis. *Curr. Protoc. Bioinforma.* **2014**, 1.12.1–34 (2014).
46. Katoh, K., Misawa, K., Kuma, K. & Miyata, T. MAFFT: a novel method for rapid multiple sequence alignment based on fast Fourier transform. *Nucleic Acids Res.* **30**, 3059–3066 (2002).
47. Emms, D. M. & Kelly, S. OrthoFinder: phylogenetic orthology inference for comparative genomics. *Genome Biol.* **20**, 238 (2019).
48. Vaidya, G., Lohman, D. J. & Meier, R. Cladistics multi-gene datasets with character set and codon information. *Cladistics* **27**, 171–180 (2011).
49. Edgar, R. C. MUSCLE: a multiple sequence alignment method with reduced time and space complexity. *BMC Bioinform.* **5**, 113 (2004).
50. Bradbury, P. J. et al. TASSEL: software for association mapping of complex traits in diverse samples. *Bioinformatics* **23**, 2633–2635 (2007).
51. Nei, M. & Li, W. H. Mathematical model for studying genetic variation in terms of restriction endonucleases. *Proc. Natl Acad. Sci. USA* **76**, 5269–5273 (1979).
52. R Core Team. R: a language and environment for statistical computing. (R Foundation for Statistical Computing, 2014); https://www.R-project.org

Acknowledgements

We thank T. Mulligan and K. Schlecht for plant care, Z. Lippman and T. Tran for comments and discussion, and C. Fugina, B. Siegel and M. Kallman for their enthusiastic involvement in some of this work. This work was supported by funding from the National Science Foundation (grant no. IOS-1546837) and from Inari Agricuture, Inc., and from the Next-Generation BioGreen 21 Program System and Synthetic Agro-biotech Center (grant no. PJ01322602) from the Rural Development Administration, Republic of Korea, Office of China Postdoctoral Affairs Fellowship (Fellowship to L.L.), and USDA NIFA Postdoctoral Fellowship (award no. 2019-67012-29654 to J.G.).

Author contributions

L.L. performed all experimental procedures except as described below, and prepared figures and co-wrote the manuscript. E.D.A., T.S. and Q.W. designed the promoter CRISPR sgRNAs and prepared the constructs for maize transformation. R.C. performed IM size measurements of the promoter CRISPR alleles. J.G. and M.B. performed the evolution analysis and co-wrote the manuscript. D.J. supervised the research and co-wrote the manuscript.

Competing interests

D.J. is a consultant with Inari, who have licensed promoter fine-tuning technology from Cold Spring Harbor Laboratory. The other authors declare no conflicts of interest.

Additional information

Supplementary information The online version contains supplementary material available at https://doi.org/10.1038/s41477-021-00858-5.

Correspondence and requests for materials should be addressed to D.J.

Peer review information *Nature Plants* thanks Scott Boden, Feng Tian, Thorsten Schnurbusch and Cristobal Uauy for their contribution to the peer review of this work.

Reprints and permissions information is available at www.nature.com/reprints.

Publisher's note Springer Nature remains neutral with regard to jurisdictional claims in published maps and institutional affiliations.

nature research

Corresponding author(s): David Jackson

Last updated by author(s): 20-Jan 2021

Reporting Summary

Nature Research wishes to improve the reproducibility of the work that we publish. This form provides structure for consistency and transparency in reporting. For further information on Nature Research policies, see our Editorial Policies and the Editorial Policy Checklist.

Statistics

For all statistical analyses, confirm that the following items are present in the figure legend, table legend, main text, or Methods section.

n/a	Confirmed	
☐	☒	The exact sample size (*n*) for each experimental group/condition, given as a discrete number and unit of measurement
☐	☒	A statement on whether measurements were taken from distinct samples or whether the same sample was measured repeatedly
☐	☒	The statistical test(s) used AND whether they are one- or two-sided *Only common tests should be described solely by name; describe more complex techniques in the Methods section.*
☒	☐	A description of all covariates tested
☒	☐	A description of any assumptions or corrections, such as tests of normality and adjustment for multiple comparisons
☐	☒	A full description of the statistical parameters including central tendency (e.g. means) or other basic estimates (e.g. regression coefficient) AND variation (e.g. standard deviation) or associated estimates of uncertainty (e.g. confidence intervals)
☐	☒	For null hypothesis testing, the test statistic (e.g. *F*, *t*, *r*) with confidence intervals, effect sizes, degrees of freedom and *P* value noted *Give P values as exact values whenever suitable.*
☒	☐	For Bayesian analysis, information on the choice of priors and Markov chain Monte Carlo settings
☒	☐	For hierarchical and complex designs, identification of the appropriate level for tests and full reporting of outcomes
☒	☐	Estimates of effect sizes (e.g. Cohen's *d*, Pearson's *r*), indicating how they were calculated

Our web collection on statistics for biologists contains articles on many of the points above.

Software and code

Policy information about availability of computer code

Data collection	Image J v1.47 was used to measure the meristem size.
Data analysis	All the statistical analysis was performed in R v3.5.3 using standard functions. The RNAseq datasets were analyzed by Trimmomatic v.0.36, TopHat v.2.1.1 and Cufflinks v2.2.1. The evolutionary analysis was performed by bedtools v2.26.0, mVISTA v1.4, MUSCLE v3.8.31, MAFFT v7, PHAST v1.5, Orthofinder v2 and TASSEL v5.

For manuscripts utilizing custom algorithms or software that are central to the research but not yet described in published literature, software must be made available to editors and reviewers. We strongly encourage code deposition in a community repository (e.g. GitHub). See the Nature Research guidelines for submitting code & software for further information.

Data

Policy information about availability of data

All manuscripts must include a data availability statement. This statement should provide the following information, where applicable:

- Accession codes, unique identifiers, or web links for publicly available datasets
- A list of figures that have associated raw data
- A description of any restrictions on data availability

Raw data for all quantifications are included as source date. The sequences of ZmFCP1 and ZmCLE7 promoter edited alleles were listed in Supplementary Table 4. The RNA-seq datasets are available from the National Center for Biotechnology Information, the ~~BioProject accessions numbers is PRJNA494874.~~

Field-specific reporting

Please select the one below that is the best fit for your research. If you are not sure, read the appropriate sections before making your selection.

☒ Life sciences ☐ Behavioural & social sciences ☐ Ecological, evolutionary & environmental sciences

For a reference copy of the document with all sections, see nature.com/documents/nr-reporting-summary-flat.pdf

Life sciences study design

All studies must disclose on these points even when the disclosure is negative.

Sample size	No sample-size calculations were performed. Sample sizes typically used in the literature for these types of experiments were also used here.
Data exclusions	No data was excluded.
Replication	For all experiments at least three independent biological replicates were performed, and all replicates were included.
Randomization	For all experiments involving phenotyping or tissue collection from plants, segregating populations and a randomized block design were used, and individuals were genotyped after planting in their final location or the genotypes were planted in a randomly distribution in the field. This ensured that all genotypes were randomized within each experiment.
Blinding	For all experiments involving phenotyping, genotypes were randomized (see randomization). Genotyping was then performed independently of any phenotyping, and the genotype was not known during phenotyping. A randomized block design was used for the phenotyping of families with known genotypes, the distribution of each family in the field was generated randomly before planting. Genotypes and phenotypes were only matched for analysis after all genotyping and phenotyping data had been collected.

Reporting for specific materials, systems and methods

We require information from authors about some types of materials, experimental systems and methods used in many studies. Here, indicate whether each material, system or method listed is relevant to your study. If you are not sure if a list item applies to your research, read the appropriate section before selecting a response.

Materials & experimental systems

n/a	Involved in the study
☒	☐ Antibodies
☒	☐ Eukaryotic cell lines
☒	☐ Palaeontology and archaeology
☒	☐ Animals and other organisms
☒	☐ Human research participants
☒	☐ Clinical data
☒	☐ Dual use research of concern

Methods

n/a	Involved in the study
☒	☐ ChIP-seq
☒	☐ Flow cytometry
☒	☐ MRI-based neuroimaging